Journal of Molecular Modeling (2018) 24:208
https://doi.org/10.1007/s00894-018-3747-z

ORIGINAL PAPER

A coarse-grained approach to studying the interactions of the antimicrobial peptides aurein 1.2 and maculatin 1.1 with POPG/POPE lipid mixtures

G. E. Balatti[1,2] · M. F. Martini[3,4] · M. Pickholz[1,2]

Received: 15 March 2018 / Accepted: 27 June 2018

Abstract

In the present work we investigated the differential interactions of the antimicrobial peptides (AMPs) aurein 1.2 and maculatin 1.1 with a bilayer composed of a mixture of the lipids 1-palmitoyl-2-oleoyl-*sn*-glycero-3-phospho-(1′-*rac*-glycerol) (POPG) and 1-palmitoyl-2-oleoyl-*sn*-glycero-3-phosphoethanolamine (POPE). We carried out molecular dynamics (MD) simulations using a coarse-grained approach within the MARTINI force field. The POPE/POPG mixture was used as a simple model of a bacterial (prokaryotic cell) membrane. The results were compared with our previous findings for structures of 1-palmitoyl-2-oleoyl-*sn*-glycero-3-phosphocholine (POPC), a representative lipid of mammalian cells. We started the simulations of the peptide–lipid system from two different initial conditions: peptides in water and peptides inside the hydrophobic core of the membrane, employing a pre-assembled lipid bilayer in both cases. Our results show similarities and differences regarding the molecular behavior of the peptides in POPE/POPG in comparison to their behavior in a POPC membrane. For instance, aurein 1.2 molecules can adopt similar pore-like structures on both POPG/POPE and POPC membranes, but the peptides are found deeper in the hydrophobic core in the former. Maculatin 1.1 molecules, in turn, achieve very similar structures in both kinds of bilayers: they have a strong tendency to form clusters and induce curvature. Therefore, the results of this study provide insight into the mechanisms of action of these two peptides in membrane leakage, which allows organisms to protect themselves against potentially harmful bacteria.

Keywords Antimicrobial peptides · Maculatin · Aurein · Coarse-grained · Molecular dynamics

Introduction

Antimicrobial peptides (AMPs) can be found in all life forms. For instance, they are a part of the innate immune system, being the first line of defense against external agents [1]. Their spectrum of applications is broad: bacteria, fungi, viruses, and eukaryotic parasites are among their targets [2, 3]. Interest in developing pharmaceutical products from such molecules is growing because AMPs exhibit potential uses in, for example, anticancer drugs [4, 5], antibiofilms [6], and immunomodulators [7, 8]. In this regard, the molecular actions of AMPs vary widely, with the action depending strongly on the peptide considered and its biological source. While many AMPs inhibit biological processes such as wall synthesis or enzyme activities [9], most interact with lipid bilayers, disrupting the integrity of membranes and in some cases achieving membrane lysis through tensioactive activity [6, 10–13].

Among the various known types of AMPs, there is an important group with well-defined characteristics: the cationic

This paper belongs to Topical Collection XIX - Brazilian Symposium of Theoretical Chemistry (SBQT2017)

Electronic supplementary material The online version of this article (https://doi.org/10.1007/s00894-018-3747-z) contains supplementary material, which is available to authorized users.

✉ M. Pickholz
mpickholz@df.uba.ar

[1] Facultad de Ciencias Exactas y Naturales, Departamento de Física, Universidad de Buenos Aires, Buenos Aires, Argentina

[2] CONICET-Universidad de Buenos Aires, IFIBA, C1428BFA Buenos Aires, Argentina

[3] Facultad de Farmacia y Bioquímica, Departamento de Farmacología, Universidad de Buenos Aires, Buenos Aires, Argentina

[4] CONICET-Universidad de Buenos Aires, IQUIMEFA, C1113AA Buenos Aires, Argentina

Published online: 17 July 2018

α-helical peptides [10, 11, 14, 15]. It has been suggested that these peptides could form amphipathic structures when interacting with bilayers [16]. Their amphipathic character, combined with their cationic charge, allows these molecules to affect membrane properties such as permeability, curvature, or thickness [15, 17].

Two main modes of action for the lytic activity of AMPs have been proposed [18]: pore formation and a "carpet-like" mechanism, whereby the AMPs disintegrate the membrane, leading to micellization. Likewise, two types of pores have been described for AMPs: a "barrel-stave" structure, with the lipid headgroups remaining in the same interfacial location; and a "toroidal" structure [19], where the headgroups of the lipids are bent, connecting both leaflets of the membrane along the pore (as illustrated in Fig. 1).

In general, eukaryotic cell membranes are less affected by the actions of this type of peptide. Such membranes are composed of zwitterionic lipids such as phosphatidylcholine (PC), phosphatidylethanolamine (PE), and sphingomyelin (SM) or neutral sterols such as cholesterol or ergosterol [20]. On the other hand, prokaryotic cells are more vulnerable to the action of AMPs, probably due to their membrane composition. Lipids such as phosphatidylglycerol (PG), cardiolipin (CL), and phosphatidylserine (PS) are among the most abundant phospholipids in bacteria [20–22]. Thus, lipids bearing a negative net charge are more abundant in prokaryotic than in eukaryotic cell membranes. This is the case for PG, which can induce the formation of cubic phases in lipid extracts from bacteria [23]. Considering the cationic character of AMPs, it is a reasonable to expect strong electrostatic interactions between these peptides and membranes. This is why the different compositions of eukaryotic and prokaryotic cell bilayers are often used to explain the bacterial selectivity of AMPs. Other factors have been identified in this selectivity in addition to electrostatic interactions, such as entropic effects [24].

In the work reported in the present paper, we focused on two cationic, amphipathic, α-helical peptides found in the skins of Australian tree frogs: aurein 1.2 (GLFDIIKKIAESF-NH2) [4] and maculatin 1.1 (GLFGVLAKVAAHVVPAIAEHF-NH2) [25]. The pairwise alignment of both sequences [26] revealed remarkable similarity at the ends along with a wide gap at the center. This gap corresponded mostly to the hydrophobic residues of maculatin 1.1 located at the center of the helix (–VAAHVVPA–). The net charge is +1 for aurein and + 1.2 for

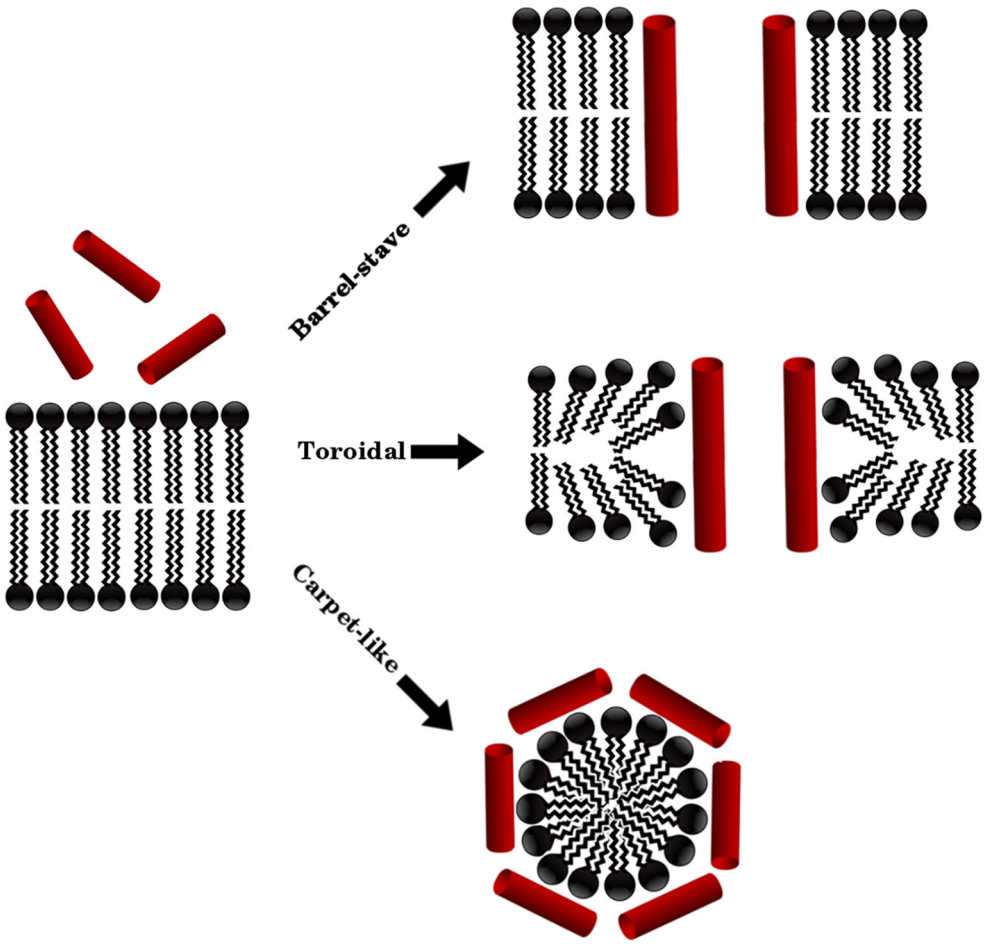

Fig. 1 Schematic representation of the mechanisms of action of AMPs

maculatin, and their average hydrophilicities on Hopp and Wood's scale [27] are 0.0 and − 0.7, respectively. In addition, the percentage of hydrophilic residues is 38% in the aurein sequence but only 10% in the maculatin one. Despite the fact that the hydrophobic moment μH (a quantitative expression of the amphipathic character) is practically the same for aurein ($\mu H = 6.77$) and maculatin ($\mu H = 6.8$), and that both peptides possess polar and nonpolar surfaces, the polar surface of maculatin is smaller than its nonpolar one, whereas both surfaces are similar in size for aurein [26].

These peptides show remarkable differences in their lytic mechanisms as well as in the peptide concentration required for maximum lytic effect, as reported in the literature [28]. On the one hand, when POPC and POPC/POPG giant unillamellar vesicles (GUVs) were exposed to maculatin 1.1, experimental evidence of pore-forming activity was reported. On the other hand, when the same vesicles were exposed to aurein 1.2, it was suggested that the "carpet" lytic mechanism acted against those liposomes. Other experimental works have provided insights into the molecular interactions of the peptides with both anionic membranes via surface plasmon resonance (SPR) spectroscopy and solid-state nuclear magnetic resonance (NMR) spectroscopy [29], or they have evaluated the insertion of peptides into PC membranes using solid-state NMR and circular dichorism (CD) [30].

In addition, molecular dynamics (MD) simulations were used to unveil details of the molecular mechanisms of action of both peptides. In MD simulations carried out with different POPC structures, aurein exhibited well-defined amphipathic behavior, forming structures compatible with pore formation (i.e., permitting water flow) [26], while maculatin induced highly curved bilayers and could form structures inside the membrane that difficult water permeation [26, 31]. The ability to induce membrane curvature could be an important effect of certain types of AMPs [32–34]. Other authors have revealed that both amidated and non-amidated forms of aurein 1.2 bind DMPC bilayers by anchoring to phenyalanine residues [35]. Moreover, atomistic simulations combined with experimental techniques suggest that the dimerization of this peptide increases its activity, changing the molecular mechanism in PC/PG membrane mixtures [36, 37].

Since the main targets of these peptides are prokaryotic cells, a difference in behavior is expected compared to bacterial membrane models. In this regard, we carried out MD simulations within the MARTINI force field in which we aimed to shed light on the mechanisms of action of these peptides. To emulate a bacterial membrane, we considered a mixture of POPG and POPE lipids. In order to identify differences between the interactions of these peptides with eukaryotic membranes and their interactions with prokaryotic membranes, we compared the results obtained here for the interactions of the peptides with a mixed POPG/POPE lipid structure to our previous results for the interactions of the peptides with POPC lipid structures.

Methods

Molecular dynamics system setup

MD simulations were performed with the GROMACS 5.0.7 [38–42] software package. CG parameters were taken from the MARTINI force field for lipids [43, 44] and amino acids (using MARTINI v.2.2p) [45], and a polarizable water (PW) model was applied [46]. The tridimensional structures of aurein 1.2 and maculatin 1.1 were taken from the Protein Data Bank [47] (codes 1VM5 [48] and 2MMJ [49], respectively). The 1VM5 structure was used unaltered for aurein 1.2, while the 2MMJ structure was modified with two point mutations (GLY to PRO and I4G to ALA) in order to obtain the wild-type maculatin 1.1 molecule. I4G corresponds to *n*-(2-methylpropyl)glycine, which is present in the NMR structure. The proline residue is an important influence on the molecular mechanism of melittin [16], a peptide which has similar structural characteristics to maculatin. Both residue modifications were achieved by editing the 3D structure directly with PyMOL [50], followed by some molecular sculpting. To generate each peptide topology, the *martinize* (v.2.6) script was used. The peptide structures were also used for secondary structure assignment, employing the Define Secondary Structure of Proteins (DSSP) program [51, 52].

Taking into account that POPG and POPE are the major anionic and zwitterionic phospholipid species found in bacteria [20], we followed the generic Gram-positive model proposed by Lee et al. [53] within the MARTINI force field. According to their model, a Gram-positive bacterium such as *Bacillus subtilis* can be represented by a membrane composed of a PG/PE (3:1) lipid mixture. Considering that experiments indicate that full vesicle leakage occurs for peptide:lipid ratios in the range 1:10 to 1:100 [28], we chose a ratio of 1:32 for our systems (see Table 1).

The membrane was built using the *insane* script [54] and carefully equilibrated by increasing the temperature from 10 to 310 K. Simulations were then carried out under the desired conditions. The properties were analyzed after ensuring that the energy, the pressure, the area per lipid, and the thickness of the bilayer had all converged. Two types of systems were considered: an *–inside* system with peptides placed inside the hydrophobic core of the membrane, and an *-outside* system with peptides placed in the aqueous phase, 3 nm away from the bilayer. The simulated systems, summarized in Table 1, were pre-equilibrated by slowly increasing the temperature and time step to the production-run conditions. Finally, MD simulations were performed with a time step of 20 fs and Coulomb/van der Waals distance cutoffs of 1.2 nm in an NP_NP_ZT ensemble using periodic boundary conditions (PBCs). The temperature was maintained at 310 K with a V-rescale thermostat [55] at a time constant of

Table 1 Simulation summary

Case	Description	System configuration	Time
Bilayer	Bilayer in water	384 POPG/128 POPE/13,110 PW/416 NA/32 CL	1 μs
Inside	32 Peptides inside the bilayer	32 PP/384 POPG/128 POPE/13,119 PW/384 NA/32 CL	2 × 1 μs 2 μs (aurein)
Outside	32 Peptides outside the bilayer	32 PP/384 POPG/128 POPE/13,119 PW/384 NA/32 CL	2 × 1 μs

1.0 ps. The pressure was coupled with a semi-isotropic Parrinello–Rahman barostat [56] (*xy* and *z* pressures were coupled independently at 1 bar) using a compressibility of 4.5×10^{-5} bar^{-1} with a time constant of 1.0 ps in a rectangular simulation box. The molecular visualization program VMD [57] was used for the snapshots. Angle distributions and mass density profiles (MDPs) were calculated with the gmx gangle and gmx density tools from the GROMACS suite. Grace [58] was used to plot all of the data obtained.

Results and discussion

We started the simulations from two different initial conditions, as discussed in the "Methods" section. By putting the peptides in water, we were able to explore their adsorption, their interactions with the lipid heads, and their indirect effects in the bilayer structure. However, as already reported in the literature, it is difficult to observe pore formation under these conditions [59]. When simulations were carried out, the peptides usually became trapped at the interface. Depending on the peptide structure, they aggregated in clusters or were adsorbed at the interface in isolation, as shown in Fig. 2. We called these cases "-outside" simulations (with the peptide name as a prefix). In order to investigate the possible peptide structures inside the bilayer, we also performed a series of simulations with the peptides initially inside the bilayer, thus bypassing the mechanism they used to get there. We called these systems "-inside" systems, with the peptide name used as a prefix.

Peptides outside the bilayer (–outside systems)

We ran simulations with 32 peptides placed in the water phase in the presence of a pre-assembled lipid bilayer. We observed that both peptides were adsorbed onto the surface comprising lipid heads; they could not access the hydrophobic region. While maculatin molecules formed clusters that were adsorbed by the membrane, aurein molecules were observed to participate in clusters or as single molecules. When simulations were started from the –outside conditions, the peptides did not penetrate any deeper than the glycerol beads.

Figure 2 shows a snapshot of the maculatin-outside system. Two aggregates formed at the surface of the bilayer and remained adsorbed over the course of the simulation. Small effects on the bilayer structure were observed, such as soft ripples.

For the aurein-outside case, all of the molecules penetrated through the interface, and peptide aggregates as well as single peptide molecules were observed. The single peptides oriented at the bilayer such that the nonpolar aminoacids faced the membrane and the polar residues faced the water (see the snapshots in Fig. S1 of the "Electronic supplementary

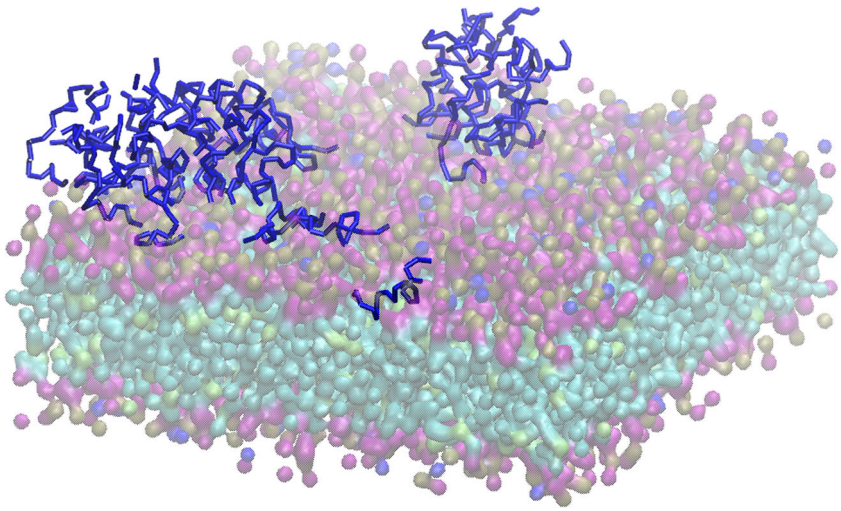

Fig. 2 Representative snapshot of the maculatin-outside system during the production run. The maculatin molecules are depicted in *blue*, and form two clusters adsorbed on the bilayer surface. Head groups of the membrane are shown in *violet* (glycerol), *ocher* (phosphate), and *blue* (amino); lipid tails are shown in *turquoise*. Simulation time of the snapshot: 512 ns

material," ESM). This behavior was also observed previously in simulations of aurein with pure POPC membranes [26].

Peptides inside the bilayer (–inside systems)

We carried out two replicate simulations of maculatin 1.1 inside the mixed POPG/POPE bilayer. The solid lines in Fig. 3a show the average MDP relative to the POPG/POPE bilayer normal (z) for the last 400 ns of the simulation. It is clear that the peptides were evenly distributed inside the POPG/POPE bilayer, but the mass density of peptides dropped markedly at the interface. For comparison, the MDP obtained during a simulation of 20 peptide molecules in a bilayer comprising 1000 POPC molecules under similar initial conditions to those used for the maculatin-inside case is also shown (dashed lines in Fig. 3a). In both the POPG/POPE and the POPC cases, maculatin 1.1 formed an aggregate inside the bilayer that remained stable during the simulation. In both bilayers, the MDP for the peptides was asymmetric, with a higher concentration observed at one of the interfaces with the water phase. This asymmetry was obtained regardless of the system size (either 1000 and 500 POPC lipids, with the same lipid:peptide ratio). In addition to this profile asymmetry, the C and N termini of the peptides showed no evidence of a preferred orientation, as can be seen in the CT/NT EDP (shown in the ESM). The absence of a preferred maculatin orientation in the POPC bilayer was also noted previously [26]. Visual inspection of the maculatin-inside simulations revealed the presence of two peptide clusters inside the POPG/POPE bilayer. Figure 3b illustrates this by displaying a representative snapshot of these peptide clusters inside the bilayer. The clusters obtained inside a POPC membrane were found to be very similar. Even though, at first glance, the POPG/POPE bilayer appeared to be very well organized (the lipid headgroups remained aligned with the xy plane), there were two or three head groups of POPG that carried water molecules and penetrated the hydrophobic core; these head groups interacted with the peptide clusters. A representative snapshot of this situation is available in Fig. S2 of the ESM.

Since AMPs are amphipathic molecules, we studied the positions of the polar and nonpolar amino acids of maculatin during the simulation trajectories. The goal was to check if the amphipathic maculatin molecules form a hydrophilic channel by orientating their nonpolar residues towards the lipid tails and their polar residues towards the interior of the cluster. As already discussed in our previous work, maculatin 1.1 has a smaller polar surface than nonpolar surface. Looking at the organization of the polar and nonpolar residues during the simulations, we observed an unstructured aggregate inside the bilayer that did not resemble a pore-like structure. A snapshot of the system taken from the top is shown in Fig. S3 of the ESM; note the lack of organization of the polar (green) and nonpolar (red) residues.

For the aurein-inside case, the MDP shows that the POPG/POPE bilayer structure was preserved during the simulation (solid lines in Fig. 4a). Peptide molecules were present all along the membrane, leading to a more symmetrical peptide distribution than seen for the maculatin-inside case. Furthermore, the density of aurein 1.2 was found to be higher at the center of the POPG/POPE bilayer than at the center of the POPC bilayer (dashed lines in Fig. 4a) [26].

Further examination of the peptides during the simulation trajectory for aurein in a POPG/POPE bilayer showed the formation of pore-like structures inside the membrane. Representative snapshots that illustrate one of these structures are shown in Fig. 4b (xz plane) and Fig. 5 (from the top of the bilayer). As we can see in Fig. 4b, the aurein molecules formed an aggregate across the membrane, connecting both

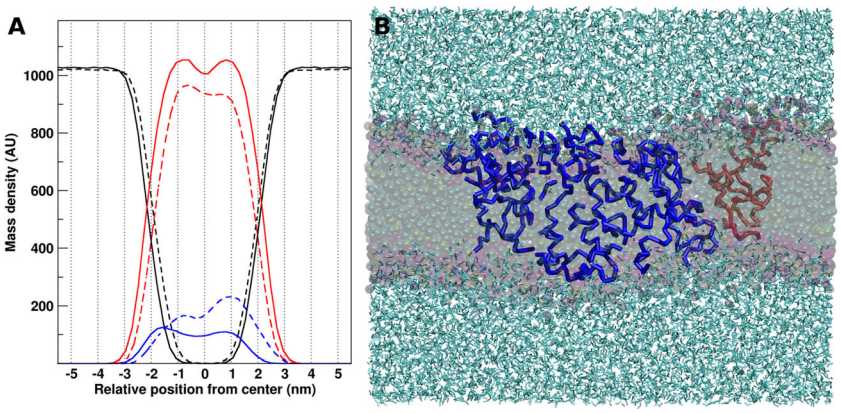

Fig. 3 **a** Mass density profile of the components in the maculatin-inside case (*solid lines*). Profiles for the water, lipids (POPG/POPE), and peptides are depicted in *black*, *red*, and *blue*, respectively. The *dashed lines* are the MDP obtained from a simulation of maculatin in a pure POPC bilayer. Peptide densities have been magnified 1.6-fold to improve visualization. **b** Representative snapshot of the POPG/POPE system with peptide clusters depicted in *blue* and *red*. Both of the clusters remained stable inside the POPG/POPE bilayer. Water molecules are colored *cyan*. The head groups of the membrane are shown in *violet* (glycerol), *ocher* (phosphate), and *blue* (amino); the lipid tails are depicted in *turquoise*. A more detailed view of the lipid headgroups in this snapshot is available in the ESM. Simulation time of the snapshot: 815.5 ns

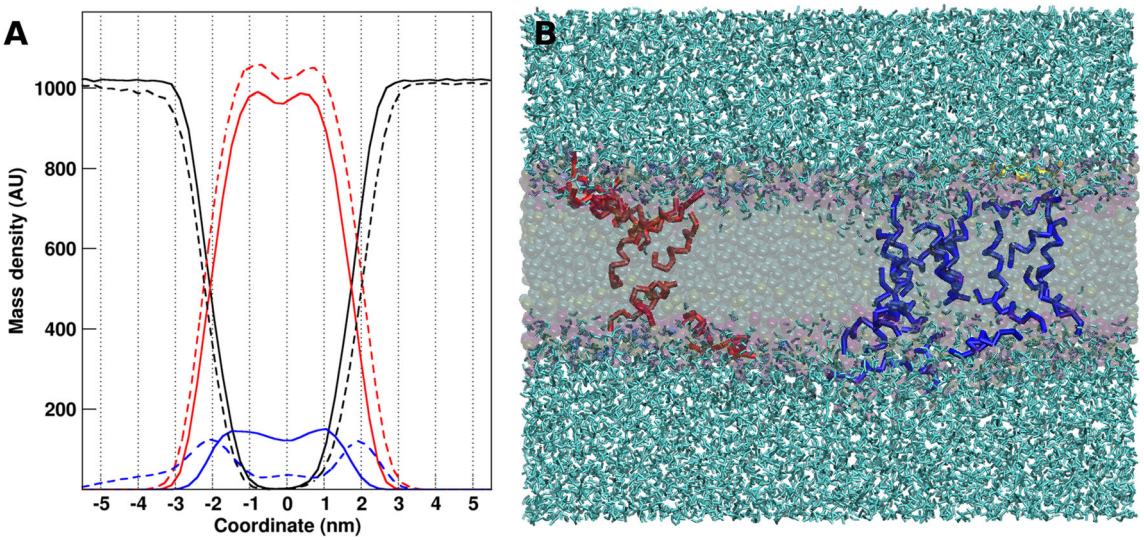

Fig. 4 **a** Mass density profile of the components in the aurein-inside case (*solid lines*). Profiles for the water, lipids, and peptides are depicted in *black*, *red*, and *blue*, respectively. The *dashed lines* are the MDP obtained from a simulation of aurein in a pure POPC bilayer. Peptide densities have been magnified 1.6-fold to improve visualization. **b** Representative snapshot of the POPG/POPE system with peptide clusters depicted in *blue* and *red*. An isolated aurein molecule is shown in *yellow* (this molecule is shown in more detail in the ESM). Both clusters remained stable inside the POPG/POPE bilayer during the simulation. It is clear that water (*cyan*) was present inside the hydrophobic core. The head groups of the membrane are shown in *violet* (glycerol), *ocher* (phosphate), and *blue* (amino); the lipid tails are depicted in *turquoise*. Simulation time of the snapshot: 550.5 ns

leaflets. The peptides adopted a pore structure that allowed small amounts of water to permeate through it. Figure 5 shows that the polar residues (in green) oriented towards the interior of the pore, while the nonpolar ones (in red) oriented towards the lipid tails. Thus, the pore-like peptide structures inside the bilayer showed considerable organization. In order to explore the organization of the terminal groups of the peptides, we calculated the MDPs of the amino-terminal (NT) and carboxy-terminal amidated (CT) groups. Figure 6a shows that the amide-terminal groups (red) were located in the hydrophobic core of the bilayer while the NT beads (blue) were positioned near to the lipid–water interfaces.

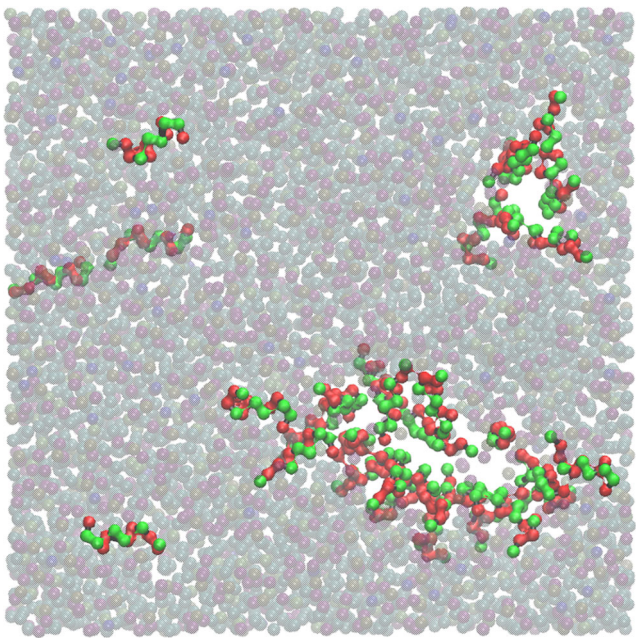

Fig. 5 Snapshot of the aurein-inside system seen from the top (*xy* bilayer plane). *Green balls* represent polar amino acids, while the *red balls* represent the nonpolar ones. Head groups of the membrane are shown in *violet* (glycerol), *ocher* (phosphate), and *blue* (amino); the lipid tails are depicted in *turquoise*. Simulation time of the snapshot: 562.5 ns

In order to garner further insight into the preferred peptide orientation with respect to the bilayer normal, we defined the vector from the NT to the CT group in a particular peptide molecule as **v**, and we measured the angle between **v** and the *xy* plane of the membrane. Note that we only considered the absolute value of this angle (for instance, 90° and − 90° were considered to be equivalent because they actually represented the same relative orientation). Figure 6b shows a histogram of average orientation angles during the simulation. For aurein, there were two preferred orientations with respect to the plane of the bilayer: ~20° and ~55°. Simulations of aurein in a POPC bilayer indicated that the aurein molecules aggregated inside the bilayer with a specific tilt angle (~20° [26]), thus forming an organized pore structure. Figure 6b also shows the results for the maculatin-inside case.

These characteristics of aurein 1.2 may be key molecular aspects of the mechanism of action of aurein. The orientation of the polar surface of aurein allows the creation of a hydrophilic channel inside a pore structure, and the preferred locations of the NT and CT groups may help aurein to span the bilayer, which therefore acts as a lipid-mimicking peptide (by contrast, maculatin does not show a preferred NT/CT orientation; see Fig. S4 in the ESM). While this behavior of aurein 1.2 is also observed to some extent in pure POPC membranes [26], when aurein molecules interact with PG/PE mixtures,

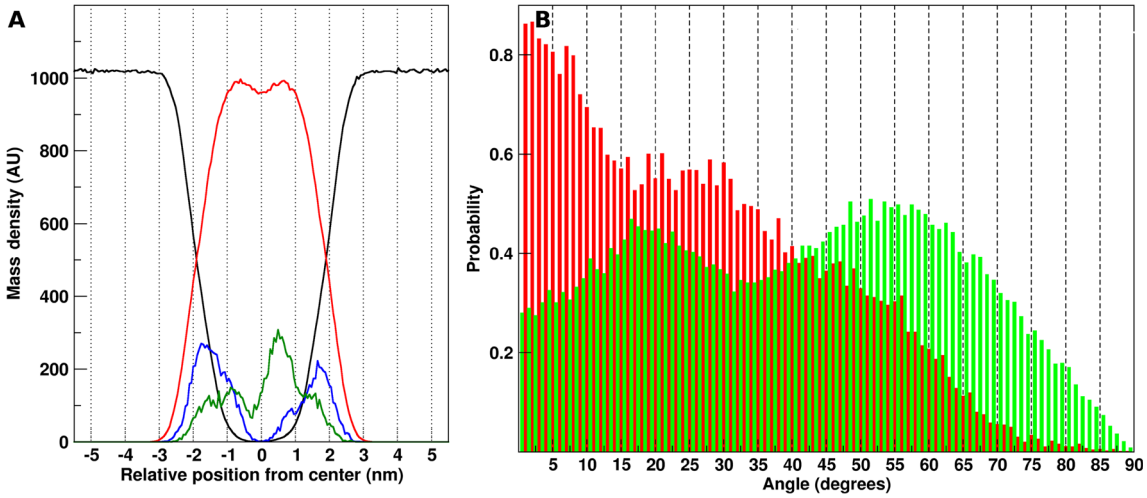

Fig. 6 **a** MDP for the components in the aurein-inside case. Amino-terminal (*blue*) and carboxy-terminal (*green*) group densities are magnified one hundredfold. Water and lipid (POPG/POPE) molecules are depicted in *black* and *red*, respectively. **b** Cumulative distribution functions for the orientations (in degrees) of aurein (green) and maculatin (red) molecules with respect to the *xy* plane

this behavior is reinforced by the proximity of the peptides to the hydrophobic core, as seen in the MDP (Fig. 4a), and the more vertical alignment of aurein molecules inside the membrane. Many molecules of water are observed inside the pore structure (Fig. 4b) even though MARTINI maps four water molecules to one bead, and despite how difficult it is to establish this kind of structure using this force field [59, 60].

Conclusions

In the work reported here, we investigated the interactions of the peptides aurein 1.2 and maculatin 1.1 with a POPG/POPE mixed lipid bilayer using coarse-grained molecular dynamics simulations. This lipid mixture was employed to emulate a bacterial membrane. We can summarize the main results obtained in this work as follows:

- Maculatin 1.1 showed a strong tendency to aggregate in water and in the membrane environment. Nevertheless, the aggregates were unstructured and preventing water permeation.
- Aurein 1.2 localized deep inside the hydrophobic region of the bacterial membrane model, adopting two possible orientations. This contrasts with the behavior of aurein in a pure POPC bilayer, where the peptide density was observed to be higher among the lipid polar headgroups, and the peptides were all oriented in the same direction.
- Although both peptides (aurein 1.2 and maculatin 1.1) formed aggregates when they were positioned inside the bilayer, only aurein 1.2 formed hydrophilic channels. The pore-like structures created by aurein show specific polar/nonpolar residue orientations and defined NT/CT-vector angles.

Our results highlighted differences between the two AMPs when they interact with a lipid mixture used as a very simple bacterial model. It should be noted, however, that bacterial membranes are very complex systems that include a wide variety of lipids and proteins. In order to construct a more realistic bacterial membrane model, our next step will be to include glycolipids in the simulations. Glycolipids play a key role in the resistance of some bacterial membranes to AMPs, as discussed by Hugo et al. [61]. Studying the link between AMP resistance and membrane composition should help to considerably boost our knowledge of the behaviors of different types of AMPs at different types of membranes, and thus the potential therapeutic effects of AMPs.

Acknowledgements This work was developed with financial support from Universidad de Buenos Aires (no. UBACYT 20020130200096BA), CONICET (nos. 0131-2014), and ANPCyT (nos. PICT-2014-3653, 2013-1205). M.F.M. and M.P. are career members of CONICET.

References

1. Wang G, Li X, Wang Z (2016) APD3: the antimicrobial peptide database as a tool for research and education. Nucleic Acids Res 44: D1087–D1093. https://doi.org/10.1093/nar/gkv1278
2. Reddy KVR, Yedery RD, Aranha C (2004) Antimicrobial peptides: Premises and promises. Int J Antimicrob Agents 24:536–547
3. Martin E, Ganz T, Lehrer RI (1995) Defensins and other endogenous peptide antibiotics of vertebrates. J Leukoc Biol 58:128–136
4. Rozek T, Wegener KL, Bowie JH et al (2000) The antibiotic and anticancer active aurein peptides from the Australian bell frogs *Litoria aurea* and *Litoria raniformis*: the solution structure of aurein 1.2. Eur J Biochem 267:5330–5341. https://doi.org/10.1046/j.1432-1327.2000.01536.x
5. Hoskin DW, Ramamoorthy A (2008) Studies on anticancer activities of antimicrobial peptides. Biochim Biophys Acta Biomembr 1778:357–375

6. de la Fuente-Núñez C, Cardoso MH, de Souza CE et al (2016) Synthetic antibiofilm peptides. Biochim Biophys Acta Biomembr 1858:1061–1069. https://doi.org/10.1016/j.bbamem.2015.12.015
7. Hilchie AL, Wuerth K, Hancock REW (2013) Immune modulation by multifaceted cationic host defense (antimicrobial) peptides. Nat Chem Biol 9:761–768. https://doi.org/10.1038/nchembio.1393
8. Mansour SC, Pena OM, Hancock REW (2014) Host defense peptides: Front-line immunomodulators. Trends Immunol 35:443–450
9. Guilhelmelli F, Vilela N, Albuquerque P et al (2013) Antibiotic development challenges: the various mechanisms of action of antimicrobial peptides and of bacterial resistance. Front Microbiol 4:353
10. Dathe M, Wieprecht T (1999) Structural features of helical antimicrobial peptides: their potential to modulate activity on model membranes and biological cells. Biochim Biophys Acta Biomembr 1462:71–87. https://doi.org/10.1016/S0005-2736(99)00201-1
11. Huang Y, Huang J, Chen Y (2010) Alpha-helical cationic antimicrobial peptides: relationships of structure and function. Protein Cell 1:143–152. https://doi.org/10.1007/s13238-010-0004-3
12. REW H, Rozek A (2002) Role of membranes in the activities of antimicrobial cationic peptides. FEMS Microbiol Lett 206:143–149
13. Jenssen H, Hamill P, Hancock REW (2006) Peptide antimicrobial agents. Clin Microbiol Rev 19:491–511
14. Tossi A, Sandri L, Giangaspero A (2000) Amphipathic, alpha-helical antimicrobial peptides. Biopolymers 55:4–30. https://doi.org/10.1002/1097-0282(2000)55:1<4::AID-BIP30>3.0.CO;2-M
15. Zelezetsky I, Tossi A (2006) Alpha-helical antimicrobial peptides—using a sequence template to guide structure–activity relationship studies. Biochim Biophys Acta Biomembr 1758:1436–1449
16. Sato H, Feix JB (2006) Peptide–membrane interactions and mechanisms of membrane destruction by amphipathic α-helical antimicrobial peptides. Biochim Biophys Acta Biomembr 1758:1245–1256. https://doi.org/10.1016/j.bbamem.2006.02.021
17. Brogden KA (2005) Antimicrobial peptides: pore formers or metabolic inhibitors in bacteria? Nat Rev Microbiol 3:238–250. https://doi.org/10.1038/nrmicro1098
18. Bahar AA, Ren D (2013) Antimicrobial peptides. Pharmaceuticals 6:1543–1575. https://doi.org/10.3390/ph6121543
19. Mihajlovic M, Lazaridis T (2010) Antimicrobial peptides in toroidal and cylindrical pores. Biochim Biophys Acta Biomembr 1798:1485–1493. https://doi.org/10.1016/j.bbamem.2010.04.004
20. Dowhan W (1997) Molecular basis for membrane phospholipid diversity: why are there so many lipids? Annu Rev Biochem 66:199–232. https://doi.org/10.1146/annurev.biochem.66.1.199
21. Goldfine H (1972) Comparative aspects of bacterial lipids. Adv Microb Physiol 8:1–58. https://doi.org/10.1016/S0065-2911(08)60187-3
22. Randle CL, Albro PW, Dittmer JC (1969) The phosphoglyceride composition of gram-negative bacteria and the changes in composition during growth. Biochim Biophys Acta Lipids Lipid Metab 187:214–220. https://doi.org/10.1016/0005-2760(69)90030-7
23. Staudegger E, Prenner EJ, Kriechbaum M et al (2000) X-ray studies on the interaction of the antimicrobial peptide gramicidin S with microbial lipid extracts: evidence for cubic phase formation. Biochim Biophys Acta Biomembr 1468:213–230. https://doi.org/10.1016/S0005-2736(00)00260-1
24. Von Deuster CIE, Knecht V (2011) Competing interactions for antimicrobial selectivity based on charge complementarity. Biochim Biophys Acta Biomembr 1808:2867–2876. https://doi.org/10.1016/j.bbamem.2011.08.005
25. Chia BCS, Carver JA, Mulhern TD, Bowie JH (2000) Maculatin 1.1, an anti-microbial peptide from the Australian tree frog, *Litoria genimaculata*. Solution structure and biological activity. Eur J Biochem 267:1894–1908. https://doi.org/10.1046/j.1432-1327.2000.01089.x
26. Balatti GE, Ambroggio EE, Fidelio GD et al (2017) Differential interaction of antimicrobial peptides with lipid structures studied by coarse-grained molecular dynamics simulations. Molecules 22:1775. https://doi.org/10.3390/molecules22101775
27. Hopp TP, Woods KR (1981) Prediction of protein antigenic determinants from amino acid sequences. Immunology 78:3824–3828. https://doi.org/10.1073/pnas.78.6.3824
28. Ambroggio EE, Separovic F, Bowie JH et al (2005) Direct visualization of membrane leakage induced by the antibiotic peptides: maculatin, citropin, and aurein. Biophys J 89:1874–1881. https://doi.org/10.1529/biophysj.105.066589
29. Gehman JD, Luc F, Hall K et al (2008) Effect of antimicrobial peptides from Australian tree frogs on anionic phospholipid membranes. Biochemistry 47:8557–8565. https://doi.org/10.1021/bi800320v
30. Marcotte I, Wegener KL, Lam YH et al (2003) Interaction of antimicrobial peptides from Australian amphibians with lipid membranes. Chem Phys Lipids 122:107–120. https://doi.org/10.1016/S0009-3084(02)00182-2
31. Bond PJ, Parton DL, Clark JF, Sansom MSP (2008) Coarse-grained simulations of the membrane-active antimicrobial peptide maculatin 1.1. Biophys J 95:3802–3815. https://doi.org/10.1529/biophysj.108.128686
32. Matsuzaki K, Sugishita KI, Ishibe N et al (1998) Relationship of membrane curvature to the formation of pores by magainin 2. Biochemistry 37:11856–11863. https://doi.org/10.1021/bi980539y
33. Schmidt NW, Wong GCL (2013) Antimicrobial peptides and induced membrane curvature: geometry, coordination chemistry, and molecular engineering. Curr Opin Solid State Mater Sci 17:151–163. https://doi.org/10.1016/j.cossms.2013.09.004
34. da Hora GCA, Archilha NL, Lopes JLS et al (2016) Membrane negative curvature induced by a hybrid peptide from pediocin PA-1 and plantaricin 149 as revealed by atomistic molecular dynamics simulations. Soft Matter 12:8884–8898. https://doi.org/10.1039/C6SM01714B
35. Shahmiri M, Enciso M, Mechler A (2015) Controls and constrains of the membrane disrupting action of Aurein 1.2. Sci Rep 5:16378. https://doi.org/10.1038/srep16378
36. Lorenzón EN, Sanches PRS, Nogueira LG et al (2013) Dimerization of aurein 1.2: effects in structure, antimicrobial activity and aggregation of *Candida albicans* cells. Amino Acids 44:1521–1528. https://doi.org/10.1007/s00726-013-1475-3
37. Lorenzón EN, Piccoli JP, Cilli EM (2014) Interaction between the antimicrobial peptide Aurein 1.2 dimer and mannans. Amino Acids 46:2627–2631. https://doi.org/10.1007/s00726-014-1832-x
38. Abraham MJ, Murtola T, Schulz R et al (2015) Gromacs: high performance molecular simulations through multi-level parallelism from laptops to supercomputers. SoftwareX 1–2:19–25. https://doi.org/10.1016/j.softx.2015.06.001
39. Van Der Spoel D, Lindahl E, Hess B et al (2005) GROMACS: fast, flexible, and free. J Comput Chem 26:1701–1718
40. Lindahl E, Hess B, van der Spoel D (2001) GROMACS 3.0: a package for molecular simulation and trajectory analysis. J Mol Model 7:306–317. https://doi.org/10.1007/s008940100045
41. Pronk S, Páll S, Schulz R et al (2013) GROMACS 4.5: a high-throughput and highly parallel open source molecular simulation toolkit. Bioinformatics 29:845–854. https://doi.org/10.1093/bioinformatics/btt055
42. Hess B, Kutzner C, Van Der Spoel D, Lindahl E (2008) GROMACS 4: algorithms for highly efficient, load-balanced, and scalable molecular simulation. J Chem Theory Comput 4:435–447. https://doi.org/10.1021/ct700301q
43. Marrink SJ, de Vries AH, Mark AE (2004) Coarse grained model for semiquantitative lipid simulations. J Phys Chem B 108:750–760. https://doi.org/10.1021/jp036508g
44. Marrink SJ, Risselada HJ, Yefimov S et al (2007) The MARTINI forcefield: coarse grained model for biomolecular simulations. J Phys Chem B 111:7812–7824
45. De Jong DH, Singh G, Bennett WFD et al (2013) Improved parameters for the MARTINI coarse-grained protein force field. J Chem Theory Comput 9:687–697. https://doi.org/10.1021/ct300646g

46. Yesylevskyy SO, Schäfer LV, Sengupta D, Marrink SJ (2010) Polarizable water model for the coarse-grained MARTINI force field. PLoS Comput Biol 6:1–17. https://doi.org/10.1371/journal.pcbi.1000810
47. Berman HM, Westbrook J, Feng Z et al (2000) The Protein Data Bank. Nucleic Acids Res 28:235–242. https://doi.org/10.1093/nar/28.1.235
48. Wang G, Li Y, Li X (2005) Correlation of three-dimensional structures with the antibacterial activity of a group of peptides designed based on a nontoxic bacterial membrane anchor. J Biol Chem 280:5803–5811. https://doi.org/10.1074/jbc.M410116200
49. Uggerhøj LE, Munk JK, Hansen PR et al (2014) Structural features of peptoid-peptide hybrids in lipid–water interfaces. FEBS Lett 588:3291–3297. https://doi.org/10.1016/j.febslet.2014.07.016
50. Schrödinger, LLC (2015) The PyMol molecular graphics system, version 1.8. Schrödinger, LLC, New York
51. Joosten RP, Te Beek TAH, Krieger E et al (2011) A series of PDB related databases for everyday needs. Nucleic Acids Res 39(Suppl 1):D411–D419. https://doi.org/10.1093/nar/gkq1105
52. Kabsch W, Sander C (1983) Dictionary of protein secondary structure: pattern recognition of hydrogen-bonded and geometrical features. Biopolymers 22:2577–2637. https://doi.org/10.1002/bip.360221211
53. Lee J, Jung SW, Cho AE (2016) Molecular insights into the adsorption mechanism of human β-defensin-3 on bacterial membranes. Langmuir 32:1782–1790. https://doi.org/10.1021/acs.langmuir.5b04113
54. Wassenaar TA, Ingólfsson HI, Böckmann RA et al (2015) Computational lipidomics with insane: a versatile tool for generating custom membranes for molecular simulations. J Chem Theory Comput 11:2144–2155. https://doi.org/10.1021/acs.jctc.5b00209
55. Bussi G, Donadio D, Parrinello M (2007) Canonical sampling through velocity rescaling. J Chem Phys 126(1):014101. https://doi.org/10.1063/1.2408420
56. Parrinello M (1981) Polymorphic transitions in single crystals: a new molecular dynamics method. J Appl Phys 52:7182. https://doi.org/10.1063/1.328693
57. Humphrey W, Dalke A, Schulten K (1996) VMD: visual molecular dynamics. J Mol Graph 14:33–38. https://doi.org/10.1016/0263-7855(96)00018-5
58. Stambulchik E (2018) Grace homepage. http://plasma-gate.weizmann.ac.il/Grace/
59. Marrink SJ, Tieleman DP (2013) Perspective on the MARTINI model. Chem Soc Rev 42:6801. https://doi.org/10.1039/c3cs60093a
60. Bennett WFD, Tieleman DP (2011) Water defect and pore formation in atomistic and coarse-grained lipid membranes: pushing the limits of coarse graining. J Chem Theory Comput 7:2981–2988. https://doi.org/10.1021/ct200291v
61. Hugo AA, Tymczyszyn EE, Gómez-Zavaglia A, Pérez PF (2012) Effect of human defensins on lactobacilli and liposomes. J Appl Microbiol 113:1491–1497. https://doi.org/10.1111/j.1365-2672.2012.05433.x